In search of a unifying theory of white matter aging: tract morphometry-microstructure relationships

Tyler D. Robinson[1], Yutong L. Sun[1], Paul T. H. Chang[1], J. Jean Chen[1,2,3]

1. Rotman Research Institute, Baycrest, Canada
2. Medical Biophysics, University of Toronto, Canada
3. Biomedical Engineering, University of Toronto, Canada

ABSTRACT

Progressive age-related changes in white matter morphometry and microstructure have been found throughout the brain. Both declines in white matter (WM) volume and deterioration of microstructural integrity have been observed. Predicting these changes across WM tracts and building an integrated model of age-related WM trajectories has proven challenging. While tractwise differences in volume and microstructural declines are common targets of investigation, there has been relatively little exploration into other attributes of tract morphology or its relation to microstructural measures in vivo. This study seeks to examine ten WM tracts for tract-wise differences in WM volume, length, the ratio of volume to length (VLR), and microstructural integrity as measured by fractional anisotropy (FA) and mean diffusivity (MD) using diffusion MRI data from the Human Connectome Project in Aging (HCP-A). From these measures, we analyzed relationships between morphometry and microstructure in the aging brain with the goal of laying the foundation for a unified model of age-related changes that relates WM microstructure/morphometry and developmental trajectories. Results indicated wide variation in rates and patterns of decline between tracts, as well as tract-specific interactions between tract VLR and microstructure. Robust sex differences were also identified. Our findings demonstrate the need for further exploration of the mechanisms behind both macro- and microstructural differences across the aging brain.

INTRODUCTION

Changes in function, structure, and microstructure in the human brain occur throughout the adult lifespan (Baker et al., 2014; Bartzokis, 2004; Bookheimer et al., 2019; Buyanova & Arsalidou, 2021; Chad et al., 2018; Kiely et al., 2022; Kodiweera et al., 2016; Piguet et al., 2009). Evidence suggests that early signs of neural degeneration can be observed in the white matter (WM) prior to their emergence in cortical regions (Debette & Markus, 2010; Hu et al., 2021; Madden et al., 2012; Seiler et al., 2018). As a result, more comprehensive modeling of age-related WM changes offers a tool to detect degeneration at earlier stages. Consistent changes in white matter structure and histology have been demonstrated in advancing age (Baker et al., 2014; Bastin et al., 2010; Choy et al., 2020; Ouyang et al., 2021; Tang et al., 1997), with overall volume decreases identified in normal aging (Bastin et al., 2010; Piguet et al., 2009; Tang et al., 1997). Notably, WM volume decreases by up to 28% in adult aging (Pakkenberg & Gundersen, 1997), but there is still a limited understanding of the microstructural variations underlying this volume reduction. In order to understand the mechanisms underlying WM decline, it is important to incorporate knowledge of age-related changes in WM morphometry and microstructure (Bartzokis, 2004; Benitez et al., 2018; Maffei et al., 2021; Yendiki et al., 2011). In turn, examining the relationship between this interaction and the WM developmental trajectory can help further elucidate the processes that govern WM degeneration in aging.

While WM volume loss in aging has been established, the regional distribution of this volume loss is as of yet under-defined. Decreases in cumulative fiber length (i.e. the total length across the brain as extrapolated from histological samples) have been observed in both humans and animals using diffusion MRI and microscopy, respectively (Baker et al., 2017; Marner et al., 2003). This loss can in part be attributed to the preferential culling of vulnerable axons, as fibers with lower axon diameter and less dense myelin sheaths are notably more vulnerable to this process (Tang et al., 1997). This further suggests that a significant contributor to WM morphometrical losses in aging may be a reduction in the total number of fibers and a concomitant increase in mean axon diameter in surviving tissue, as opposed to changes in the length of surviving axons. As WM fibers with higher diameter are also typically higher in length (Liewald et al., 2014), aging tracts should demonstrate increases in length relative to volume as shorter, narrower fibers are culled and the longer surviving fibers comprise a greater portion of the WM tissue. However, to what degree this potential effect contributes to changes in WM volume, considering the general atrophy of brain volume with age (Azevedo et al., 2019; Fjell et al., 2009, 2014; Sala et al., 2012), is unclear. Individual fiber tracts in the white matter exhibit varying degrees of vulnerability to age-related fiber culling (Choy et al., 2020), potentially giving rise to previous observations of both

decreasing and increasing fiber length in specific major white matter bundles including the splenium and superior longitudinal fasciculus (Ouyang et al., 2021), calling into question the assumption that overall decreases in fiber length correspond to regional decreases in tract length. Moreover, the tools with which living WM can be accurately delineated into discrete tracts are both relatively new and continually improving (Maffei et al., 2021). Only recently have trackwise regional differences in the WM been accessible for modeling small structural changes in vivo. morphometrical research has noted cross-sectional tract-wise differences in age-related decline with regards to volume and microstructure (Bastin et al., 2010; Choy et al., 2020), but in the context of aging, it is also important to assess normalized fibre length in order to account for sex differences and age-related general atrophy, thereby gleaning the proportional instead of absolute changes in different WM tracts (Bajada et al., 2019).

To expand beyond morphometric observations, diffusion MRI metrics such as fractional anisotropy (FA) and mean diffusivity (MD) offer proxy measures for WM microstructural integrity (Madden et al., 2012; Stadlbauer et al., 2008). Culling of axonal fibers and demyelination of surviving axons results in measurable changes in diffusion, such that mean diffusivity increases and fractional anisotropy decreases as axon bundles become less dense (Choy et al., 2020; Fan et al., 2019; Kodiweera et al., 2016). Declines in microstructural integrity in aging WM are associated with both WM hyperintensities and implicated in declining cognitive performance (Debette & Markus, 2010; Hu et al., 2021). Existing research has also identified diverging patterns of decline in different WM regions, such as sections of the corpus callosum, and broader anterior and posterior regions of the brain (Armstrong et al., 2004; Brickman et al., 2012; Fan et al., 2019; Kiely et al., 2022; Seiler et al., 2018). Regional differences in microstructural decline are therefore of considerable interest for anticipating pathological changes (Debette & Markus, 2010). However, the tracts addressed across studies vary considerably.

We reasonably expect microstructural variations to underlie morphometrical variations in aging (Armstrong et al. 2004; Baker et al. 2014; Choy et al. 2020), but interaction between morphometrical and microstructural declines represents another sparsely addressed topic (Bastin et al., 2010; Kezele et al., 2008; Seiler et al., 2018). Prior investigation notes a decrease in overall fibers with age that could account for measurable changes in WM volume (Marner et al., 2003). This would pose microstructural declines as a direct cause of morphometrical changes in volume. However, histological findings also note that surviving WM fibers are thicker with advancing age. Moreover, while age may result in lower density in fiber bundles (Choy et al., 2020; Fan et al., 2019; Kiely et al., 2022; Marner et al., 2003), changes in density may not necessitate uniform decreases in volume, as space within fiber bundles is occupied by intercellular fluid (Kodiweera et al., 2016). Uncertainty in these processes make it difficult to anticipate the relationships between microstructural decline and changing WM morphometry with age, necessitating further observation and modeling.

This study sought to map changes in WM morphometry and microstructure, examine their interactions, and compare those changes across ten WM tracts. Tractwise microstructural declines with age, assessed using FA and MD, and are used as the anchoring metrics of this study. One of the novelties of our approach is to parse WM morphometry into volume, length and the ratio of the two. These are, in turn, compared to the microstructural measures. We hypothesize that: (1) given patterns of preferential WM fiber culling (Marner et al., 2003; Tang et al., 1997), and associations between axon diameter and axon length (Liewald et al., 2014), advancing age will be associated with higher mean tract length relative to the size of the brain, i.e., that tracts become relatively "thinner" with age; (2) microstructural differences will be present in those tracts that demonstrate age-related morphometrical differences based on the theory that age-related declines in WM integrity precede changes in WM microstructure; and (3) that age-related microstructural differences will be greatest in tracts which demonstrate greatest age-related morphometrical differences.

METHODS

Subjects and data acquisition

This study involved data from five hundred and thirty-five healthy adult subjects (300 female, aged 36-100 years) of the Human Connectome Project in Aging (HCP-A) dataset (OMB Control# 0925-0667) (Bookheimer et al., 2019; Harms et al., 2018). Of this sample, thirty-two subjects were excluded due to MRI artifacts resulting in notable errors when producing WM masks. An additional three subjects (100 years of age) were excluded as outliers. This resulted in a final sample size of 500 subjects (294 female, aged 36-89). All subjects were in good health and without pathological cognitive impairment (i.e. stroke, clinical dementia).

Each data set included a whole-brain T1-weighted structural MRI (0.8 mm isotropic resolution) and diffusion-weighted MRI (dMRI), collected on one of four matched Siemens Prisma 3T MRI scanners, with a 1.5 mm isotropic voxel resolution, MB=4, with 93 directions at b=1500s/mm^2. Further parameters for structural and diffusion image acquisition can be found in (Harms et al., 2018).

Image analysis

dMRI data were corrected for eddy-current and susceptibility-related distortions via EDDY. Diffusion data were used to identify and reconstruct eighteen major white matter tracts using the Tracts Constrained by Underlying Anatomy (TRACULA) tool in Freesurfer version 7.2.0. FMRIB Software Library version 6.0.5 (FSL)'s fslmaths function was then used to produce per subject masks of each WM tract in local space. A 99th percentile voxelwise apparent diffusion coefficient (ADC) intensity threshold was applied to the generated tracts to exclude potential outliers, followed by a 20% threshold on the resulting masks to

generate the final masked regions of interest (ROI) used throughout this study. The eighteen reconstructed tracts were collapsed bilaterally to produce ten tracts of interest: The forceps major (Fmajor), forceps minor (Fminor), anterior thalamic radiation (ATR), Cingulum Angular Bundle (CAB), Cingulate Gyrus (CCG), Corticospinal Tract (CST), Inferior Longitudinal Fasciculus (ILF), Superior Longitudinal Fasciculus Parietal (SLFP), Superior Longitudinal Fasciculus Temporal (SLFT), and the Uncinate Fasciculus (UNC). In single tract analyses, Rosner's tests were performed to identify and exclude volume outliers per tract. The resulting subject counts were as follows: Fmajor (N=493), Fminor (N=493), ATR (N=497), CAB (N=490), CCG (N=495), CST (N=491), ILF (N=497), SLFP (N=497), SLFT (N=495), and UNC (N=495).

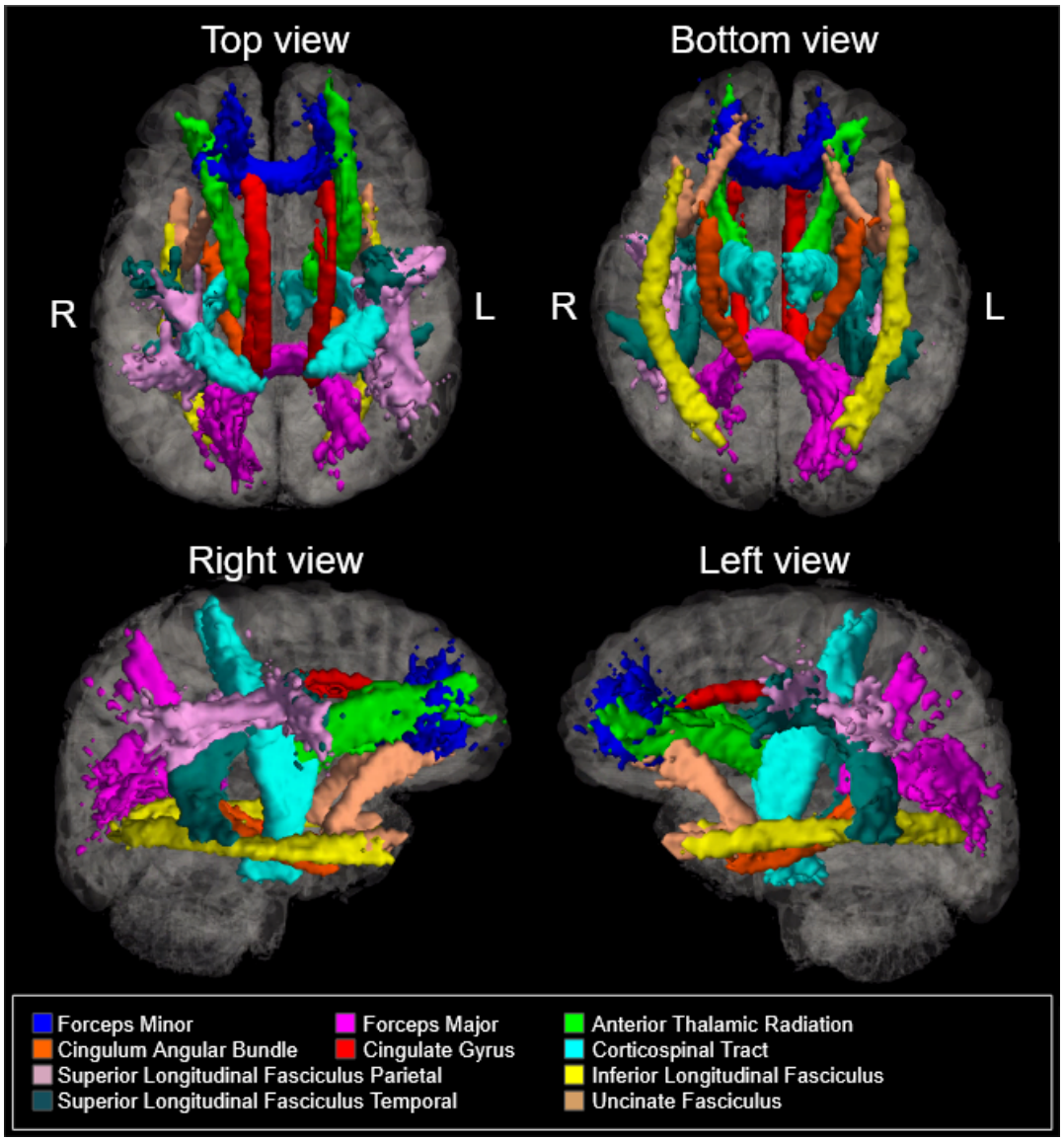

Figure 1. Ten bilateral tracts of interest reconstructed in Freesurfer's TRACULA package

Morphometry

From these masked regions, morphometry measures were calculated for tract volume, length, and volume-to-length ratio (VLR):

1. Tract volume:
    a. Raw tract volume ("Volume"): calculated as the total number of voxels ($2x2x2mm^3$) included in each masked tract region.
    b. Normalized tract volume ("$Volume_{norm}$"): calculated as tract volume divided by subject-specific intracranial volumes (ICV). This represents the tract volume as a percentage of the brain volume, thereby reducing the effect of inherent inter-subject variability in tissue volumes.
2. Tract length
    a. Raw tract length ("Length"): calculated as the mean streamline length from 1500 streamlines per tract in TRACULA.
    b. Normalized tract length ("$Length_{norm}$"): the raw tract length divided by the length of an subject-specific length of age-stable white matter tract (the cingulate gyrus (CCG)), as identified from its relatively stable raw tract length identified in the raw values. This reduces the effect of inherent inter-subject variability in tract lengths.
3. Tract volume-to-length ratio (VLR)
    a. Raw VLR ("VLR"): calculated as the ratio of tract volume to length. This represents the "thinness" of a tract relative to a reference tissue.
    b. Normalized VLR ("VLR_{norm}"): calculated as the ratio of ICV-corrected tract volume to CCG-corrected tract length. This represents the "thinness" of a tract relative to a reference tissue.

Microstructure

FA and MD maps were derived using Dipy's DKI tool, to provide kurtosis-corrected DTI metrics (given the high b-value used in the HCP-A dMRI acquisitions). Tract masks generated in the morphometrical assessment were applied to the local space diffusion images using fslmaths to generate mean fractional anisotropy (FA) and mean diffusivity (MD) values for each tract of interest of each participant.

Statistical analyses

Whole-brain morphometry

In these analyses we assessed the relationships between morphometry, age and sex using multivariate regression. All analyses in this study were conducted in R (version 4.1.1). First, age was

regressed separately onto whole-WM mean $Length_{norm}$, whole-WM total $Volume_{norm}$, and whole-WM mean VLR_{norm} using sex as a covariate of no interest. Subsequent assessment of sex differences in mean morphometry was conducted via sequential multivariate regressions of sex onto mean tract length, total tract volume, and mean tract VLR using age as a covariate of no interest.

Whole-brain microstructure

Whole-brain age-related microstructure differences were assessed via multivariate regression by first regressing age onto mean MD and mean FA using sex as a covariate of no interest. Subsequent assessment of sex differences in microstructure was conducted via sequential multivariate regressions of sex on to mean MD and mean FA, using age as a covariate of no interest.

Tract-wise morphometry

Following whole-brain WM analyses, age was regressed onto tractwise $Length_{norm}$, $Volume_{norm}$, and VLR_{norm} values for each of the ten reconstructed tracts. As in the whole-brain analyses, sex was used as a covariate of no interest. Subsequent multivariate regressions of sex onto normalized morphometric values were performed, using age as a covariate of no interest. False detection rate (FDR) adjustment was applied to all resulting p-values to correct for multiple comparisons.

Tract-wise microstructure

Sequential multivariate regressions were also used to assess tractwise age-related differences in microstructure, with age regressed onto MD/FA for each of the ten tracts using sex as a covariate of no interest. Sex was subsequently regressed onto MD/FA for each of the ten tracts using age as a regressor of no interest. FDR adjustment was again applied to the resulting p-values.

Morphometry vs. microstructure

Three multivariate regression models were constructed to assess the relationships between morphometry, microstructure, age, and sex in our sample. These models were first applied to "whole-brain" mean $Length_{norm}$, total $Volume_{norm}$, and mean VLR_{norm}, then to the individual values for each tract of interest:

- *Model 1. microstructure vs. morphometry across ages:* assesses the degree to which morphometric metrics account for the age-related variability in mean normalized tract length, volume, and VLR, with subject sex as a covariate of no interest. That is,
    - $\{FA, MD\} = f(Length_{norm}+Sex)$
    - $\{FA_t, MD\} = f(VLR_{norm}+Sex)$

- *Model 2. microstructure vs. morphometry between sexes:* assess the degree to which morphometric metrics account for sex-related differences in normalized tract length, volume and VLR, with subject age as a covariate of no interest. That is,
    - {FA, MD} = f($Length_{norm}$+Age)
    - {FA, MD} = f(VLR_{norm}+Age)
    - One set of models is produced for each sex.
- *Model 3. microstructure vs. morphometry regardless of sex:* incorporated sex and age as regressors of interest into Model 1, along with interaction effects. Fractional length, volume, and VLR, along with age and sex, were regressed onto MD/FA. That is,
    - {FA, MD} = f($Length_{norm}$+Sex+Age+$Length_{norm}$*Age+Sex*Age)
    - {FA, MD} = f(VLR_{norm}+Sex+Age+$Length_{norm}$*Age+Sex*Age)

RESULTS

Whole-Brain Morphometry

Age Differences:

Negative associations were observed between age and both normalized whole-brain mean tract length ($F(2, 497) = 66.8$, $p < .001$, $R^2_{Adjusted} = .21$, slope = -0.1mm/year) and normalized whole-brain mean volume ($F(2, 497) = 84.9$, $p < .001$, $R^2_{Adjusted} = .25$, slope = 684 mm^3/year) when controlling for sex. Similarly, age and normalized tract VLR are significantly and negatively associated ($F(2, 497) = 72.4$, $p < .001$, $R^2_{Adjusted} = .22$, slope = 0.64 mm^3/mm/year).

Sex Differences:

Male subjects demonstrated greater normalized tract length ($F(2, 497) = 66.8$, $p < .001$, $R^2_{Adjusted} = .21$, effect = 3.0mm), volume ($F(2, 497) = 84.9$, $p < .001$, $R^2_{Adjusted} = .25$, effect = 38941.6 mm^3), and VLR values ($F(2, 497) = 72.4$, $p < .001$, $R^2_{Adjusted} = .22$, effect = 51.2 mm^3/mm) across tracts.

Tractwise Morphometry

Morphometry vs. Age:

Negative relationships between age and normalized tract length were identified in Fminor, CAB, CST, ILF, SLFP, SLFT, and UNC. Negative relationships between age and normalized tract volume were identified in Fmajor, Fminor, ATR, CAB, CCG, ILF, SLFP, SLFT, and UNC. Negative tractwise relationships between age and normalized tract VLR were observed in the Fmajor, the Fminor, ATR, CAB, CCG, and UNC (Figure 2).

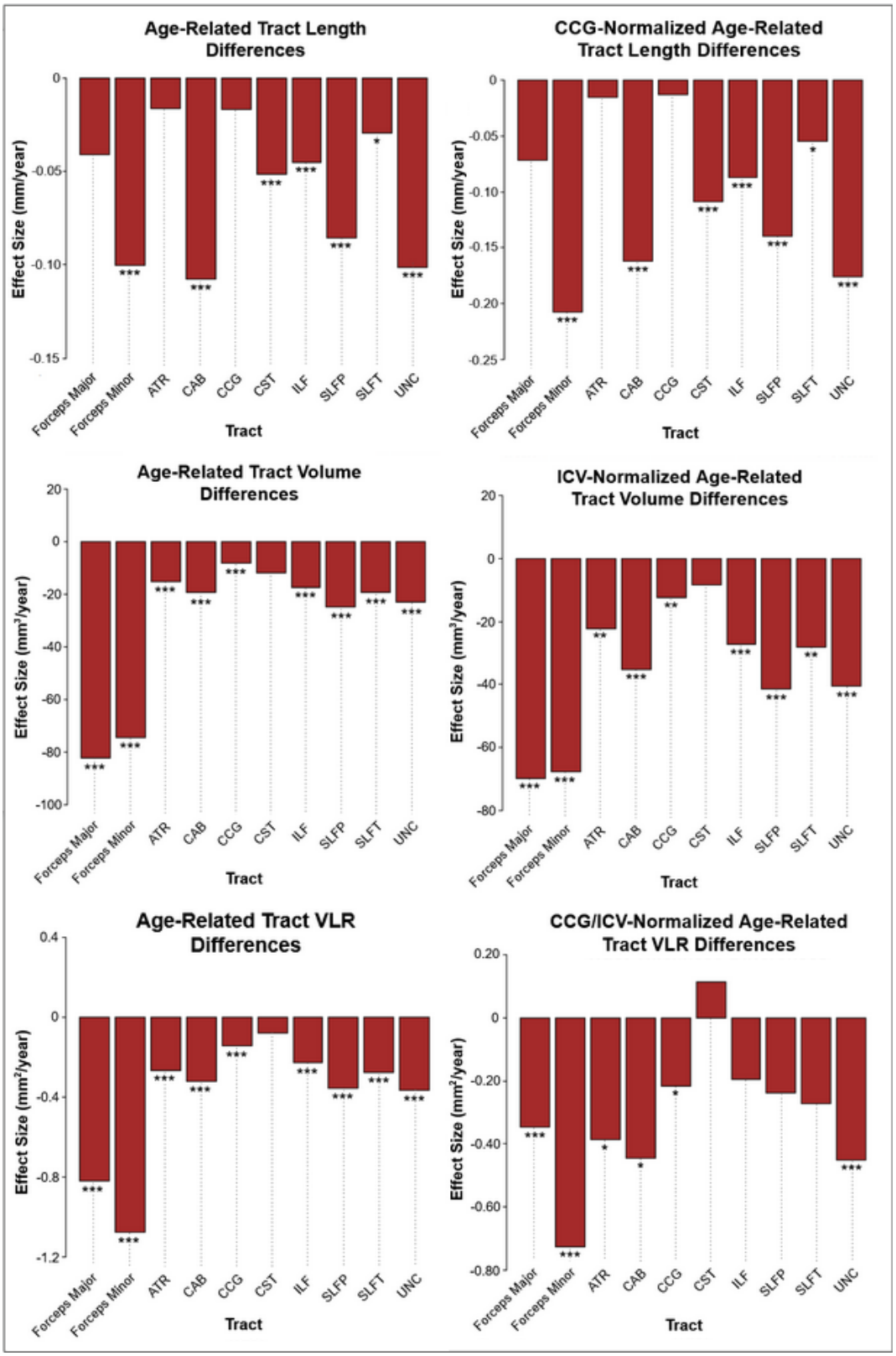

Figure 2. Tractwise relationships between age and WM length, volume, and VLR using raw (left) and normalized (right) measures.

Morphometry vs. Sex:

Female subjects demonstrated higher normalized tract length in the CST, while male subjects demonstrated higher normalized length in the Fmajor, Fminor, ATR, CCG, ILF, SLFP, SLFT, and UNC. Male subjects also showed significantly higher normalized volume and VLR in all ten tracts of interest (Figure 3).

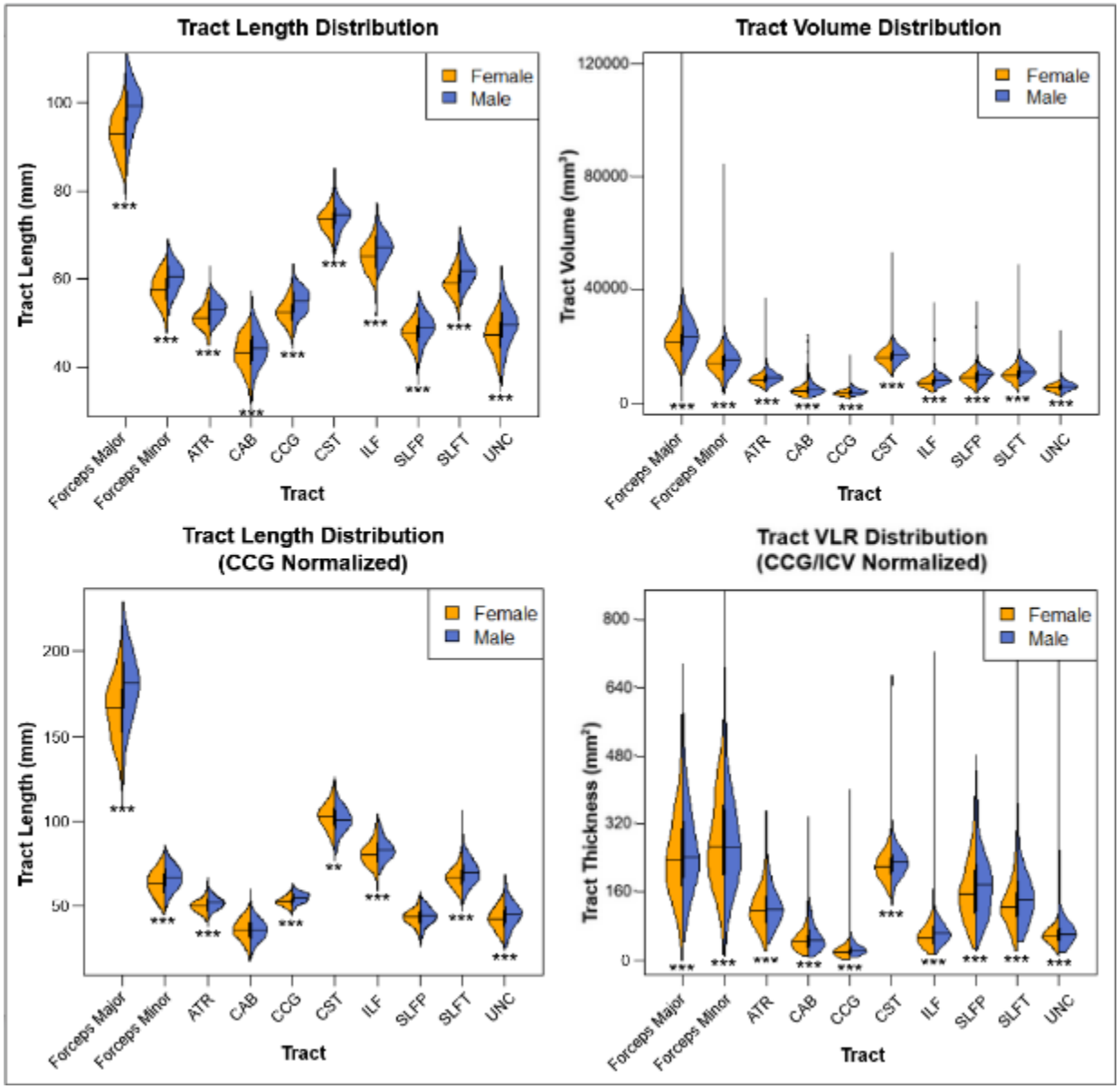

Figure 3. Tractwise distributions of raw tract length, raw tract volume, CCG normalized tract length, and CCG/ICV normalized tract VLR in male and female participants.

Whole-Brain Microstructure

MD/FA vs. Age/Sex:

Age demonstrated a significant positive association with mean MD ($F(2, 497) = 77.8$, $p < .001$, $R^2_{Adjusted} = .24$), with mean WM MD increasing by 1.1 mm^2/s per year of age. Age also demonstrated a significant negative association with mean FA ($F(2, 497) = 11.6$, $p < .001$, $R^2_{Adjusted} = .04$), such that the value of mean WM FA decreased by 4.1 per year of age. No relationships between sex and whole-brain MD/FA were observed.

Tractwise Microstructure

MD/FA vs. Age:

All ten tracts of interest showed significant positive relationships between age and MD. Age was significantly negatively related to FA in the Fmajor, Fminor, ATR, CAB, CCG, ILF, and SLFP.

MD/FA vs. Sex:

Female subjects demonstrated significantly higher MD in the CST ($F(2, 497) = 47.0$, $p < .001$, $R^2_{Adjusted} = .16$, effect = 0.000028 mm^2/s) and in the UNC ($F(2, 497) = 71.2$, $p < .001$, $R^2_{Adjusted} = .22$, effect = 0.0000076 mm^2/s) In the ILF, men demonstrated significantly higher MD ($F(2, 497) = 63.3$, $p < .001$, $R^2_{Adjusted} = .20$, effect = 0.0000067 mm^2/s). In the CAB, female subjects demonstrated significantly higher FA ($F(2, 497) = 14.0$, $p < .001$, $R^2_{Adjusted} = .05$, effect = 0.011). In the UNC, male subjects demonstrated significantly higher FA ($F(2, 497) = 3.1$, $p = .046$, $R^2_{Adjusted} = .008$, effect = 0.0063).

Whole-brain morphometry-Microstructure Relationships

Model 1 (morphometry vs. microstructure):

Mean normalized tract length was significantly negatively associated with MD ($F(2, 497) = 75.6$, $p = .013$, $R^2_{Adjusted} = .01$, effect = -0.00000097). No other significant whole-brain relationships were identified.

Model 2 (Sex differences in morphometry-microstructure relationships):

No whole-brain relationships were observed between microstructural measures and either normalized tract length or normalized tract VLR after dividing the sample by sex.

Model 3 (Interaction amongst morphometry, age, sex and microstructure):

Normalized tract length vs. MD and FA: a significant positive interaction effect between sex, age, and FA was identified when controlling for length ($F(2, 494) = 5.8$, $p < .001$, $R^2_{Adjusted} = .05$, effect = 0.00042). Female subjects showed significantly higher FA when controlling for length and age ($F(2, 494) = 5.8$, $p < .001$, $R^2_{Adjusted} = .05$, effect = 0.024). A significant relationship between age and MD was also observed when controlling for mean tract length and sex ($F(2, 494) = 5.8$, $p < .001$, $R^2_{Adjusted} = .05$, effect = 0.0000032 mm^2/s per year).

Normalized tract VLR vs. MD and FA: a significant positive interaction effect was identified between VLR, age, and MD when controlling for sex was identified ($F(2, 494) = 33.6$, $p < .001$, $R^2_{\text{Adjusted}} = .25$, effect = 0.000000027). Significant associations were observed between age and MD when controlling for VLR and sex ($F(2, 494) = 33.6$, $p < .001$, $R^2_{\text{Adjusted}} = .25$, effect = 0.0000020 mm^2/s per year), and between age and FA when controlling for VLR and sex ($F(2, 494) = 33.3$, $p < .001$, $R^2_{\text{Adjusted}} = .24$, effect = -0.00094 FA per year).

Tractwise morphometry-Microstructure Relationships

Model 1 (morphometry vs. microstructure):

Normalized tract length vs. MD and FA: significant negative associations with MD were identified in Fminor and SLFP, and a significant positive association in ATR. Significant positive associations with FA were identified in Fminor, CAB, CST, and ILF, while a single significant negative association was identified in the UNC.

Normalized tract VLR vs. MD and FA: significant negative associations were identified in the Fmajor, Fminor, ATR, CST, and UNC, and a significant positive association in the CAB. Significant negative associations with FA were identified in the CAB, while in the SLFP and SLFT, significant positive associations with FA were identified (Table 1).

Model 2 (Sex differences in morphometry-microstructure relationships):

Normalized tract length vs. MD and FA: a significant positive association with MD was identified in female subjects in the Fmajor and ATR. Female subjects demonstrated significant positive relationships between length and FA in the CST and the ILF, in addition to a significant negative association in the UNC, while male subjects demonstrated a significant negative association in the SLFP.

Normalized tract VLR vs. MD and FA: both female and male subjects demonstrated significant positive associations between VLR and MD in the CAB, with male subjects showing additional significant negative associations in the Fmajor and CST. Both sexes demonstrated significant negative associations between VLR and FA in the Fmajor and CAB, along with a significant positive association in the SLFT. Female subjects showed an additional significant positive association with FA in the SLFP, while male subjects demonstrated a significant negative association in the Fminor (Table 2).

Model 3 (Interaction amongst morphometry, age, sex and microstructure):

Normalized tract length vs. MD and FA: a significant negative interaction effect was identified between length, age, and MD in the SLFP. A significant positive association between length and MD when controlling for sex and age was observed in the SLFP. Significant positive associations between age and MD when controlling for length and sex were also observed in both the SLFP and the UNC.

Normalized tract VLR vs. MD and FA: significant negative interaction effects between VLR, age, and MD were identified in the Fmajor, ATR, and CCG. A significant positive relationship between VLR and MD when controlling for age and sex was observed in the CCG. Additionally, significant positive associations between age and MD when controlling for VLR and sex were observed in the Fmajor, Fminor, ATR, CCG, ILF, SLFP, SFLT, and UNC (Table 3).

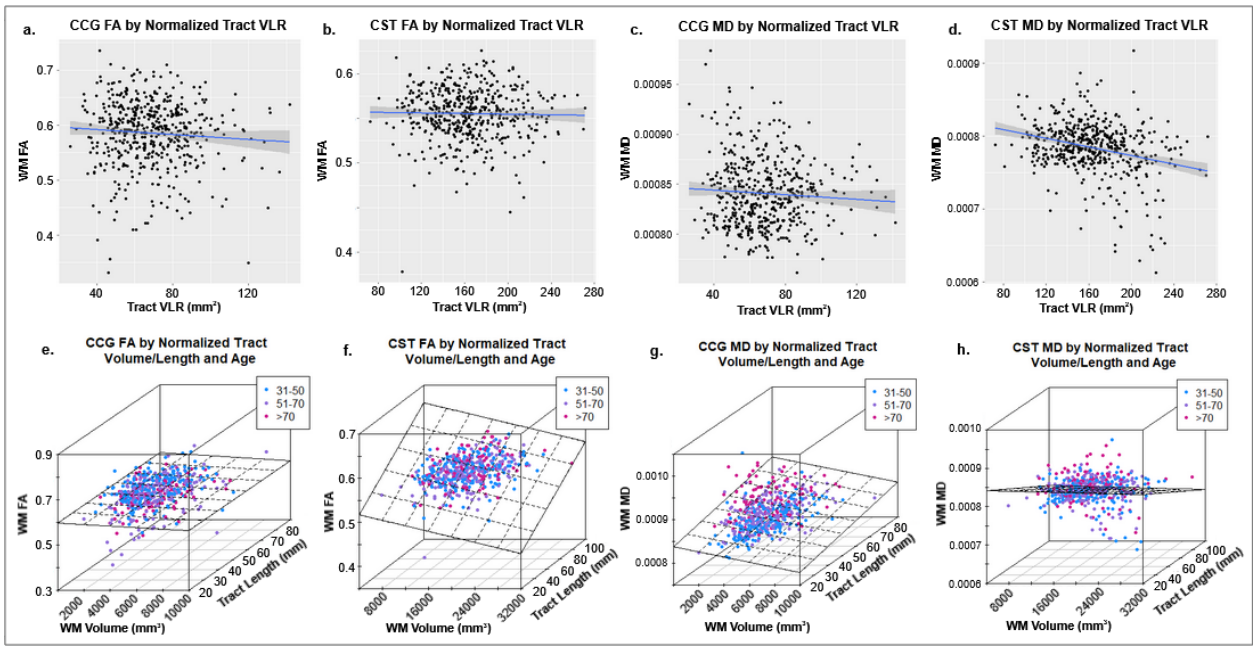

Figure 4. Comparison of tractwise relationships between VLR_{norm} and FA in the CCG (a) and CST (b), VLR_{norm} and MD in the CCG (c) and CST (d), FA, $Volume_{norm}$, and $Length_{norm}$ in the CCG (e) and CST (f), and MD, $Volume_{norm}$ and $Length_{norm}$ in the CCG (g) and CST (h) demonstrating variation in patterns of morphology-microstructure relationships between tracts.

DISCUSSION

Our initial hypotheses posited that (1) WM tracts would become thinner with age (as represented by a decrease in the normalized tract VLR with age), driven by selective survival of larger and hence longer fibers; (2) tracts exhibiting morphometrical differences with age would also demonstrate microstructural differences with age; and (3) the magnitude of age-related microstructural differences would correspond with magnitude of morphometrical differences across different tracts. Our first hypothesis was supported, but not due to normalized tract length increases with age (driven by apparent survival bias). Moreover, the relationships pertaining to the remaining hypotheses were demonstrated to be highly variable across the brain, rather than following consistent patterns across tracts per our hypotheses.

Whole-brain age and morphometry:

We started our analyses with raw (unnormalized) tract volume and length, and in line with existing research, advancing age was associated with overall decreases in raw tract volume. This fits the current understanding that white matter volume atrophies with age. Similarly, raw tract length was noted to decrease with age as well. This was anticipated in raw length values due to the expected shrinking of the white matter outpacing any potential increases in normalized tract length.

To account for inter-individual differences in head size, we normalized the tract volumes by intracranial volume, and tract length by the CCG, the tract demonstrating the least age-related length variation. Thus, the normalized VLR would represent a minimally biased metric of the "thinness" of the tracts.

Negative associations between age and normalized tract length were observed, countering our initial expectation that tracts become proportionately longer in aging. Moreover, similar to raw WM volume, ICV-normalized tract volume continued to show decreases with age. Thus, normalized VLR decreased in the majority of regions of interest, supporting the general hypothesis that tracts mainly become thinner with age.

Tractwise age and morphometry:

Tractwise patterns in morphometry were considerably more varied than those suggested by whole-brain analyses. Tractwise analysis of raw volume differences with age showed decreasing raw tract volume with age in all tested tracts with the exception of the CST. Even in those tracts that did demonstrate age-related declines, some tracts, specifically the forceps major and forceps minor, exhibited notably greater age-related raw volume differences than other WM regions. Wide variability in age-related differences were also noted in the raw length analyses, with seven tracts showing varying degrees of age-related differences and three (forceps major, ATR, and CCG) showing no significant differences (Figure X). The CCG, due to the observed age stability in its length, recommended itself as the normalization target in subsequent tract length analyses.

Analysis of tractwise normalized VLR measures indicates considerable variation in shapes of tracts in aging. Age-related differences in normalized VLR were found in six of ten tracts, however, the ILF, SLFP, and SLFT demonstrated no association between age and normalized VLR. Additionally, the CST was notable as having no identified relationships between age and either normalized VLR or normalized tract volume. Considering these exceptions cumulatively, only three tracts of interest, the Fminor, CAB, and UNC, demonstrated age effects on all three morphometrical values assessed.

One possibility is that per-tract morphometrical changes fundamentally differ in their patterns of decline. This would suggest that a tract like the CST, which has demonstrated age-related differences in normalized length without corresponding changes in normalized volume or VLR, does in fact shorten

with age without considerable losses in volume. In contrast, a tract like the CCG would be expected to demonstrate the opposite pattern, narrowing with age as it loses volume without corresponding losses in tract length. This model of variable morphometry changes by tract depicts an aging brain that alters considerably in its shape and volume distribution as age-related declines progress. However, this interpretation does not address why each tract shortens or narrows, nor does it clarify whether a lack of declines in volume represents a greater resistance to deterioration or an absence of underlying deteriorating influences.

Whole-brain age, morphometry and microstructure:

*R*elationships between tractwise micro- and macrostructure in our findings were similarly varied to those observed in the macrostructure alone. Initial whole-brain observations of the relationships between age and WM integrity note the expected trends of increasing MD and decreasing FA with advancing age. This mirrors general findings in the literature regarding microstructural WM decline (Benitez et al., 2018; Sala et al., 2012).

Targeted analyses of the interactions between microstructure and macrostructure revealed a more complex set of differences than suggested by the microstructural results. Whole-brain trends from Models 1 and 3 suggest that higher MD values were associated with lower normalized tract lengths. Additionally, Model 3 identified interactions between the age-MD association and normalized tract length as well as normalized VLR. These results suggest that morphometrical differences may predict regional resilience to age-related declines, or otherwise represent regions in which microstructural declines have not yet impacted morphometry. However, these morphometry effects were not observed in analyses of FA.

Tractwise age, morphometry, and microstructure

Tractwise comparisons broadly followed the same trends observed in the whole-brain analysis, with notable exceptions in the absence of age effects on FA in the CST, SLFT, and UNC. These three tracts all exhibited different morphometrical patterns with age, as the CST was observed to only differ in normalized length, while the SLFT differed in normalized length and normalized volume without corresponding differences in normalized VLR and the UNC showed age effects on all three morphometric measures.

Relationships between micro-and macrostructure were highly varied across the brain with regards to age effects. A continued absence of whole-brain morphometry-FA associations was also observed in Model 3 despite the presence of morphometry-MD associations. Nonetheless, Models 1 and 2 did identify associations between normalized length, normalized VLR and FA in individual tracts when controlling for sex and age, respectively. This suggests that the micro-macrostructural associations are influenced by age and sex in a tract-specific manner. As different tracts exhibit different patterns of age-related declines, and

which tracts exhibit which patterns appear to vary by sex, a unified model relating morphometry and microstructure in the aging brain will need to incorporate systematic regional variations.

The CCG and CST represent notable outliers in the tracts of interest addressed by this study. The CST is both one of the first recognizable tracts in early brain development and one of the first to myelinate (Grotheer et al., 2022; H. Huang et al., 2009). In our study, it was also the only tract to not demonstrate changes in normalized volume, VLR and FA in aging, suggesting a considerable resilience to both macro- and micro-structural declines. In contrast, the CCG exhibited the strongest age associations with FA as well as robust age effects on both tract volume and VLR, but no age effects on tract length. It is also the only tract to demonstrate significant interactions between tract VLR, age, and MD (Model 3). These two tracts are thus strong candidates for more targeted investigation into the mechanisms of interaction between morphometry and microstructural integrity as they differ across regions.

Another interpretation of the tractwise morphometric differences models variability in age-related differences as a cross-sectional observation of stages in an ongoing process. This model suggests that potential causes of age-related declines are shared across the brain, but take effect at different ages or progress at different rates between tracts. As such, a tract like the CST might show age-related declines in volume considerably later, or at a considerably slower rate, than a tract like the CCG. This model better fits the hypothesis that changes in morphometry are driven by common declines in WM integrity, which themselves may progress at different regional rates. However, the presence of both tracts that exhibit normalized length losses without normalized volume losses and those that exhibit the inverse, suggests the presence of additional factors influencing tractwise resilience to at least one axis of morphometry. I.e., if differences in normalized volume declines are cross-sectional observations of the same pattern, differences in normalized length declines must be influenced by an additional factor, or vice versa. Otherwise, a shared underlying cause for changes in morphometry could not explain inverse patterns between normalized volume and normalized length with age.

Conclusions

Both morphometry and microstructure analyzed in this study depict WM age-related differences as highly tract-specific and difficult to compress into a set of simplified trends. Broad whole-brain effects supported our expectations for normalized volume and length decreases with age, along with anticipated microstructural declines. Examining VLR revealed additional patterns in age-related WM change consistent with our predictions. To our knowledge, this is the first study to incorporate in-vivo WM tract length differences in healthy aging.

Complicating the task of modeling age-related WM changes is the apparent presence of additional factors in determining which tracts exhibit specific patterns of decline. These trends cannot be fully

accounted for by observed micro-/macrostructural interactions. Additional microstructural and histological variables will need to be incorporated into future models. An area of considerable interest to this study is the exploration of WM perfusion. Imaging of regional perfusion in the WM is a relatively novel capability with observed relationships to WM integrity (Chen et al., 2013; Kim et al., 2020). Regional differences in WM perfusion may represent a missing piece in our understanding of age-related WM declines as a whole.

REFERENCES

Armstrong, C. L., Traipe, E., Hunter, J. V., Haselgrove, J. C., Ledakis, G. E., Tallent, E. M., Shera, D., & van Buchem, M. A. (2004). Age-related, regional, hemispheric, and medial-lateral differences in myelin integrity in vivo in the normal adult brain. *AJNR. American Journal of Neuroradiology*, *25*(6), 977–984.

Azevedo, C. J., Cen, S. Y., Jaberzadeh, A., Zheng, L., Hauser, S. L., & Pelletier, D. (2019). Contribution of normal aging to brain atrophy in MS. *Neurology(R) Neuroimmunology & Neuroinflammation*, *6*(6). https://doi.org/10.1212/NXI.0000000000000616

Bajada, C. J., Schreiber, J., & Caspers, S. (2019). Fiber length profiling: A novel approach to structural brain organization. *NeuroImage*, *186*, 164–173.

Baker, L. M., Laidlaw, D. H., Cabeen, R., Akbudak, E., Conturo, T. E., Correia, S., Tate, D. F., Heaps-Woodruff, J. M., Brier, M. R., Bolzenius, J., Salminen, L. E., Lane, E. M., McMichael, A. R., & Paul, R. H. (2017). Cognitive reserve moderates the relationship between neuropsychological performance and white matter fiber bundle length in healthy older adults. *Brain Imaging and Behavior*, *11*(3), 632–639.

Baker, L. M., Laidlaw, D. H., Conturo, T. E., Hogan, J., Zhao, Y., Luo, X., Correia, S., Cabeen, R., Lane, E. M., Heaps, J. M., Bolzenius, J., Salminen, L. E., Akbudak, E., McMichael, A. R., Usher, C., Behrman, A., & Paul, R. H. (2014). White matter changes with age utilizing quantitative diffusion MRI. *Neurology*, *83*(3), 247–252.

Bartzokis, G. (2004). Age-related myelin breakdown: a developmental model of cognitive decline and Alzheimer's disease. *Neurobiology of Aging*, *25*(1), 5–18; author reply 49–62.

Bastin, M. E., Muñoz Maniega, S., Ferguson, K. J., Brown, L. J., Wardlaw, J. M., MacLullich, A. M. J., & Clayden, J. D. (2010). Quantifying the effects of normal ageing on white matter structure using unsupervised tract shape modelling. *NeuroImage*, *51*(1), 1–10.

Benitez, A., Jensen, J. H., Falangola, M. F., Nietert, P. J., & Helpern, J. A. (2018). Modeling white matter

tract integrity in aging with diffusional kurtosis imaging. *Neurobiology of Aging*, *70*, 265–275.

Bookheimer, S. Y., Salat, D. H., Terpstra, M., Ances, B. M., Barch, D. M., Buckner, R. L., Burgess, G. C., Curtiss, S. W., Diaz-Santos, M., Elam, J. S., Fischl, B., Greve, D. N., Hagy, H. A., Harms, M. P., Hatch, O. M., Hedden, T., Hodge, C., Japardi, K. C., Kuhn, T. P., … Yacoub, E. (2019). The Lifespan Human Connectome Project in Aging: An overview. *NeuroImage*, *185*, 335–348.

Brickman, A. M., Meier, I. B., Korgaonkar, M. S., Provenzano, F. A., Grieve, S. M., Siedlecki, K. L., Wasserman, B. T., Williams, L. M., & Zimmerman, M. E. (2012). Testing the white matter retrogenesis hypothesis of cognitive aging. *Neurobiology of Aging*, *33*(8), 1699–1715.

Buyanova, I. S., & Arsalidou, M. (2021). Cerebral White Matter Myelination and Relations to Age, Gender, and Cognition: A Selective Review. *Frontiers in Human Neuroscience*, *15*, 662031.

Chen, J. J., Rosas, H. D., & Salat, D. H. (2013). The relationship between cortical blood flow and sub-cortical white-matter health across the adult age span. *PloS One*, *8*(2), e56733.

Choy, S. W., Bagarinao, E., Watanabe, H., Ho, E. T. W., Maesawa, S., Mori, D., Hara, K., Kawabata, K., Yoneyama, N., Ohdake, R., Imai, K., Masuda, M., Yokoi, T., Ogura, A., Taoka, T., Koyama, S., Tanabe, H. C., Katsuno, M., Wakabayashi, T., … Sobue, G. (2020). Changes in white matter fiber density and morphology across the adult lifespan: A cross-sectional fixel-based analysis. *Human Brain Mapping*, *41*(12), 3198–3211.

Debette, S., & Markus, H. S. (2010). The clinical importance of white matter hyperintensities on brain magnetic resonance imaging: systematic review and meta-analysis. *BMJ* , *341*, c3666.

Fan, Q., Tian, Q., Ohringer, N. A., Nummenmaa, A., Witzel, T., Tobyne, S. M., Klawiter, E. C., Mekkaoui, C., Rosen, B. R., Wald, L. L., Salat, D. H., & Huang, S. Y. (2019). Age-related alterations in axonal microstructure in the corpus callosum measured by high-gradient diffusion MRI. *NeuroImage*, *191*, 325–336.

Fjell, A. M., McEvoy, L., Holland, D., Dale, A. M., Walhovd, K. B., & Alzheimer's Disease Neuroimaging Initiative. (2014). What is normal in normal aging? Effects of aging, amyloid and Alzheimer's disease on the cerebral cortex and the hippocampus. *Progress in Neurobiology*, *117*,

20–40.

Fjell, A. M., Walhovd, K. B., Fennema-Notestine, C., McEvoy, L. K., Hagler, D. J., Holland, D., Brewer, J. B., & Dale, A. M. (2009). One-year brain atrophy evident in healthy aging. *The Journal of Neuroscience: The Official Journal of the Society for Neuroscience*, *29*(48), 15223–15231.

Genc, S., Smith, R. E., Malpas, C. B., Anderson, V., Nicholson, J. M., Efron, D., Sciberras, E., Seal, M. L., & Silk, T. J. (2018). Development of white matter fibre density and morphology over childhood: A longitudinal fixel-based analysis. *NeuroImage*, *183*, 666–676.

Grotheer, M., Rosenke, M., Wu, H., Kular, H., Querdasi, F. R., Natu, V. S., Yeatman, J. D., & Grill-Spector, K. (2022). White matter myelination during early infancy is linked to spatial gradients and myelin content at birth. *Nature Communications*, *13*(1), 997.

Harms, M. P., Somerville, L. H., Ances, B. M., Andersson, J., Barch, D. M., Bastiani, M., Bookheimer, S. Y., Brown, T. B., Buckner, R. L., Burgess, G. C., Coalson, T. S., Chappell, M. A., Dapretto, M., Douaud, G., Fischl, B., Glasser, M. F., Greve, D. N., Hodge, C., Jamison, K. W., … Yacoub, E. (2018). Extending the Human Connectome Project across ages: Imaging protocols for the Lifespan Development and Aging projects. *NeuroImage*, *183*, 972–984.

Huang, H., Xue, R., Zhang, J., Ren, T., Richards, L. J., Yarowsky, P., Miller, M. I., & Mori, S. (2009). Anatomical characterization of human fetal brain development with diffusion tensor magnetic resonance imaging. *The Journal of Neuroscience: The Official Journal of the Society for Neuroscience*, *29*(13), 4263–4273.

Huang, S. Y., Tian, Q., Fan, Q., Witzel, T., Wichtmann, B., McNab, J. A., Daniel Bireley, J., Machado, N., Klawiter, E. C., Mekkaoui, C., Wald, L. L., & Nummenmaa, A. (2020). High-gradient diffusion MRI reveals distinct estimates of axon diameter index within different white matter tracts in the in vivo human brain. *Brain Structure & Function*, *225*(4), 1277–1291.

Hu, H.-Y., Ou, Y.-N., Shen, X.-N., Qu, Y., Ma, Y.-H., Wang, Z.-T., Dong, Q., Tan, L., & Yu, J.-T. (2021). White matter hyperintensities and risks of cognitive impairment and dementia: A systematic review and meta-analysis of 36 prospective studies. *Neuroscience and Biobehavioral Reviews*, *120*, 16–27.

Kezele, I. B., Arnold, D. L., & Collins, D. L. (2008). Atrophy in white matter fiber tracts in multiple sclerosis is not dependent on tract length or local white matter lesions. *Multiple Sclerosis* , *14*(6), 779–785.

Kiely, M., Triebswetter, C., Cortina, L. E., Gong, Z., Alsameen, M. H., Spencer, R. G., & Bouhrara, M. (2022). Insights into human cerebral white matter maturation and degeneration across the adult lifespan. *NeuroImage*, *247*, 118727.

Kim, C.-M., Alvarado, R. L., Stephens, K., Wey, H.-Y., Wang, D. J. J., Leritz, E. C., & Salat, D. H. (2020). Associations between cerebral blood flow and structural and functional brain imaging measures in individuals with neuropsychologically defined mild cognitive impairment. *Neurobiology of Aging*, *86*, 64–74.

Kodiweera, C., Alexander, A. L., Harezlak, J., McAllister, T. W., & Wu, Y.-C. (2016). Age effects and sex differences in human brain white matter of young to middle-aged adults: A DTI, NODDI, and q-space study. *NeuroImage*, *128*, 180–192.

Lebel, C., & Beaulieu, C. (2011). Longitudinal development of human brain wiring continues from childhood into adulthood. *The Journal of Neuroscience: The Official Journal of the Society for Neuroscience*, *31*(30), 10937–10947.

Liewald, D., Miller, R., Logothetis, N., Wagner, H.-J., & Schüz, A. (2014). Distribution of axon diameters in cortical white matter: an electron-microscopic study on three human brains and a macaque. *Biological Cybernetics*, *108*(5), 541–557.

Madden, D. J., Bennett, I. J., Burzynska, A., Potter, G. G., Chen, N.-K., & Song, A. W. (2012). Diffusion tensor imaging of cerebral white matter integrity in cognitive aging. *Biochimica et Biophysica Acta*, *1822*(3), 386–400.

Maffei, C., Lee, C., Planich, M., Ramprasad, M., Ravi, N., Trainor, D., Urban, Z., Kim, M., Jones, R. J., Henin, A., Hofmann, S. G., Pizzagalli, D. A., Auerbach, R. P., Gabrieli, J. D. E., Whitfield-Gabrieli, S., Greve, D. N., Haber, S. N., & Yendiki, A. (2021). Using diffusion MRI data acquired with ultra-high gradients to improve tractography in routine-quality data. In *bioRxiv* (p.

2021.06.28.450265). https://doi.org/10.1101/2021.06.28.450265

Marner, L., Nyengaard, J. R., Tang, Y., & Pakkenberg, B. (2003). Marked loss of myelinated nerve fibers in the human brain with age. *The Journal of Comparative Neurology*, *462*(2), 144–152.

Ouyang, Y., Cui, D., Yuan, Z., Liu, Z., Jiao, Q., Yin, T., & Qiu, J. (2021). Analysis of Age-Related White Matter Microstructures Based on Diffusion Tensor Imaging. *Frontiers in Aging Neuroscience*, *13*, 664911.

Pakkenberg, B., & Gundersen, H. J. (1997). Neocortical neuron number in humans: effect of sex and age. *The Journal of Comparative Neurology*, *384*(2), 312–320.

Piguet, O., Double, K. L., Kril, J. J., Harasty, J., Macdonald, V., McRitchie, D. A., & Halliday, G. M. (2009). White matter loss in healthy ageing: a postmortem analysis. *Neurobiology of Aging*, *30*(8), 1288–1295.

Sala, S., Agosta, F., Pagani, E., Copetti, M., Comi, G., & Filippi, M. (2012). Microstructural changes and atrophy in brain white matter tracts with aging. *Neurobiology of Aging*, *33*(3), 488–498.e2.

Seiler, S., Fletcher, E., Hassan-Ali, K., Weinstein, M., Beiser, A., Himali, J. J., Satizabal, C. L., Seshadri, S., DeCarli, C., & Maillard, P. (2018). Cerebral tract integrity relates to white matter hyperintensities, cortex volume, and cognition. *Neurobiology of Aging*, *72*, 14–22.

Slater, D. A., Melie-Garcia, L., Preisig, M., Kherif, F., Lutti, A., & Draganski, B. (2019). Evolution of white matter tract microstructure across the life span. *Human Brain Mapping*, *40*(7), 2252–2268.

Stadlbauer, A., Salomonowitz, E., Strunk, G., Hammen, T., & Ganslandt, O. (2008). Age-related degradation in the central nervous system: assessment with diffusion-tensor imaging and quantitative fiber tracking. *Radiology*, *247*(1), 179–188.

Stassart, R. M., Möbius, W., Nave, K.-A., & Edgar, J. M. (2018). The Axon-Myelin Unit in Development and Degenerative Disease. *Frontiers in Neuroscience*, *12*, 467.

Tang, Y., Nyengaard, J. R., Pakkenberg, B., & Gundersen, H. J. (1997). Age-induced white matter changes in the human brain: a stereological investigation. *Neurobiology of Aging*, *18*(6), 609–615.

Yeatman, J. D., Wandell, B. A., & Mezer, A. A. (2014). Lifespan maturation and degeneration of human

brain white matter. *Nature Communications*, *5*, 4932.

Yendiki, A., Panneck, P., Srinivasan, P., Stevens, A., Zöllei, L., Augustinack, J., Wang, R., Salat, D., Ehrlich, S., Behrens, T., Jbabdi, S., Gollub, R., & Fischl, B. (2011). Automated probabilistic reconstruction of white-matter pathways in health and disease using an atlas of the underlying anatomy. *Frontiers in Neuroinformatics*, *5*, 23.

Yu, Q., Peng, Y., Kang, H., Peng, Q., Ouyang, M., Slinger, M., Hu, D., Shou, H., Fang, F., & Huang, H. (2020). Differential White Matter Maturation from Birth to 8 Years of Age. *Cerebral Cortex* , *30*(4), 2673–2689.

Tables

Table 1: Model 1 - Tractwise Length/VLR Relationships with Microstructure (Covaried for Sex)

	Normalized Length (mm)		**Normalized VLR** (mm^2)	
Tract	FA	MD (mm^2/sec)	FA	MD (mm^2/sec)
Fmajor	$F(2, 490) = 2.0$, $p = .13$, $R^2_{Adjusted} = .004$	$F(2, 490) = 6.1$, $p = .002$, $R^2_{Adjusted} = .02$	$F(2, 490) = 18.1$, $p < .001$, $R^2_{Adjusted} = .06$	$F(2, 490) = 12.2$, $p < .001$, $R^2_{Adjusted} = .04$
	-0.00013	0.00000018	**-0.0080*** **	**-0.0000056*** **
Fminor	$F(2, 490) = 8.7$, $p < .001$, $R^2_{Adjusted} = .03$	$F(2, 490) = 12.0$, $p < .001$, $R^2_{Adjusted} = .04$	$F(2, 490) = 1.7$, $p = .18$, $R^2_{Adjusted} = .003$	$F(2, 490) = 12.2$, $p < .001$, $R^2_{Adjusted} = .04$
	0.0087* **	**-0.0000012*** **	-0.00156	**-0.0000035** **
ATR	$F(2, 494) = 2.2$, $p = .11$, $R^2_{Adjusted} = .005$	$F(2, 494) = 5.5$, $p < .001$, $R^2_{Adjusted} = .02$	$F(2, 494) = 1.6$, $p = .21$, $R^2_{Adjusted} = .002$	$F(2, 494) = 4.5$, $p = .012$, $R^2_{Adjusted} = .01$
	0.00048	**0.0000014** **	-0.00033	**-0.0000020** **
CAB	$F(2, 487) = 9.7$, $p < .001$, $R^2_{Adjusted} = .03$	$F(2, 487) = 1.3$, $p = .002$, $R^2_{Adjusted} = .001$	$F(2, 487) = 38.6$, $p < .001$, $R^2_{Adjusted} = .13$	$F(2, 487) = 16.8$, $p < .001$, $R^2_{Adjusted} = .06$
	0.0011 **	-0.000000094	**-0.008*** **	**0.0000044*** **
CCG	$F(2, 492) = 2.2$, $p = .11$, $R^2_{Adjusted} = .005$	$F(2, 492) = 1.1$, $p = .32$, $R^2_{Adjusted} = .0006$	$F(2, 492) = 38.6$, $p < .16$, $R^2_{Adjusted} = .004$	$F(2, 492) = 1.1$, $p = .35$, $R^2_{Adjusted} = .0002$
	0.0012	-0.00000075	-0.0023	-0.0000019
CST	$F(2, 488) = 8.1$, $p < .001$, $R^2_{Adjusted} = .03$	$F(2, 488) = 36.4$, $p < .001$, $R^2_{Adjusted} = .13$	$F(2, 488) = 0.86$, $p = .41$, $R^2_{Adjusted} = -.0005$	$F(2, 488) = 41.1$, $p < .001$, $R^2_{Adjusted} = .14$
	0.00063* **	-0.00000022	-0.00064	**-0.0000024** **
ILF	$F(2, 494) = 9.2$, $p < .001$, $R^2_{Adjusted} = .03$	$F(2, 494) = 3.0$, $p = .05$, $R^2_{Adjusted} = .0008$	$F(2, 494) = 0.89$, $p = .41$, $R^2_{Adjusted} = -.0004$	$F(2, 488) = 4.3$, $p = .014$, $R^2_{Adjusted} = .01$
	0.0089* **	-0.000000049	-0.00136	-0.0000020

SLFP	$F(2, 494) = 1.6$, $p = .20$, $R^2_{Adjusted} = .002$	$F(2, 494) = 12.5$, $p < .001$, $R^2_{Adjusted} = .04$	$F(2, 494) = 5.8$, $p = .003$, $R^2_{Adjusted} = .02$	$F(2, 494) = 1.1$, $p = .33$, $R^2_{Adjusted} = .0004$
	-0.00045	**-0.0000016*** **	**0.0013** **	-0.00000068
SLFT	$F(2, 492) = 2.5$, $p = .08$, $R^2_{Adjusted} = .006$	$F(2, 492) = 1.3$, $p = .26$, $R^2_{Adjusted} = .001$	$F(2, 492) = 8.6$, $p < .001$, $R^2_{Adjusted} = .03$	$F(2, 492) = 2.2$, $p = .12$, $R^2_{Adjusted} = .005$
	0.00033	0.00000013	**0.0022*** **	-0.0000010
UNC	$F(2, 492) = 10.1$, $p < .001$, $R^2_{Adjusted} = .04$	$F(2, 492) = 3.7$, $p = .02$, $R^2_{Adjusted} = .01$	$F(2, 492) = 3.0$, $p = .05$, $R^2_{Adjusted} = .008$	$F(2, 492) = 6.3$, $p = .002$, $R^2_{Adjusted} = .02$
	-0.00074* **	-0.00000042	-0.0000088	**-0.0000028** **

Table 2: Model 2 - Tractwise Sex Differences Relationships Between Length/VLR and Microstructure (Covaried for Age)

	Normalized Length (mm)				**Normalized VLR** (mm^2)			
	FA		MD (mm^2/sec)		FA		MD (mm^2/sec)	
Tract	Female	Male	Female	Male	Female	Male	Female	Male
Fmajor	$F(2, 287) = 4.7$, $p = .009$, $R^2_{Adjusted} = .02$	$F(2, 200) = 2.1$, $p = .13$, $R^2_{Adjusted} = .01$	$F(2, 287) = 34.0$, $p < .001$, $R^2_{Adjusted} = .19$	$F(2, 200) = 9.9$, $p < .001$, $R^2_{Adjusted} = .08$	$F(2, 287) = 16.5$, $p < .001$, $R^2_{Adjusted} = .10$	$F(2, 200) = 11.6$, $p < .001$, $R^2_{Adjusted} = .10$	$F(2, 287) = 31.8$, $p < .001$, $R^2_{Adjusted} = .18$	$F(2, 200) = 12.1$, $p < .001$, $R^2_{Adjusted} = .10$
	-0.0002	-0.000068	**0.00000021***	0.00000018	**-0.0192*** **	**-0.1408*** **	-0.00000392	**-0.0000096***
Fminor	$F(2, 288) = 22.3$, $p < .001$, $R^2_{Adjusted} = .13$	$F(2, 199) = 11.1$, $p < .001$, $R^2_{Adjusted} = .00$	$F(2, 288) = 76.7$, $p < .001$, $R^2_{Adjusted} = .34$	$F(2, 199) = 26.7$, $p < .001$, $R^2_{Adjusted} = .20$	$F(2, 288) = 23.1$, $p < .001$, $R^2_{Adjusted} = .13$	$F(2, 199) = 21.3$, $p < .001$, $R^2_{Adjusted} = .17$	$F(2, 288) = 76.7$, $p < .001$, $R^2_{Adjusted} = .34$	$F(2, 199) = 26.9$, $p < .001$, $R^2_{Adjusted} = .20$
	0.00020	0.00036	0.00000014	-0.000000092	-0.0036	**-0.0112*** **	-0.00000112	0.00000176
ATR	$F(2, 289) = 6.2$, $p = .002$, $R^2_{Adjusted} = .03$	$F(2, 202) = 0.17$, $p = .85$, $R^2_{Adjusted} = -.008$	$F(2, 289) = 79.5$, $p < .001$, $R^2_{Adjusted} = .35$	$F(2, 202) = 34.1$, $p < .001$, $R^2_{Adjusted} = .25$	$F(2, 289) = 5.5$, $p = .004$, $R^2_{Adjusted} = .03$	$F(2, 202) = 0.3$, $p = .71$, $R^2_{Adjusted} = -.007$	$F(2, 289) = 65.7$, $p < .001$, $R^2_{Adjusted} = .31$	$F(2, 202) = 32.3$, $p < .001$, $R^2_{Adjusted} = .23$
	0.00063	0.00022	**0.0000025*** **	0.00000082	-0.000656	-0.0012	-0.00000028	-0.00000044
CAB	$F(2, 285) = 9.1$, $p < .001$, $R^2_{Adjusted} = .05$	$F(2, 199) = 4.1$, $p = .018$, $R^2_{Adjusted} = .03$	$F(2, 285) = 14.8$, $p < .001$, $R^2_{Adjusted} = .09$	$F(2, 199) = 2.4$, $p < .001$, $R^2_{Adjusted} = .10$	$F(2, 285) = 28.3$, $p < .001$, $R^2_{Adjusted} = .16$	$F(2, 199) = 25.1$, $p < .001$, $R^2_{Adjusted} = .19$	$F(2, 285) = 22.1$, $p < .001$, $R^2_{Adjusted} = .13$	$F(2, 199) = 14.0$, $p < .001$, $R^2_{Adjusted} = .11$
	0.00075	0.00043	0.00000059	0.00000022	**-0.0184*** **	**-0.0168*** **	**0.0000096*** **	**0.0000088**
CCG	$F(2, 289) = 15.1$, $p < .001$,	$F(2, 200) = 4.8$, $p = .009$,	$F(2, 289) = 40.1$, $p < .001$,	$F(2, 200) = 19.2$, $p < .001$,	$F(2, 289) = 15.4$, $p < .001$,	$F(2, 200) = 6.1$, $p = .003$,	$F(2, 289) = 40.1$, $p < .001$,	$F(2, 200) = 18.5$, $p < .001$,

	$R^2_{Adjusted}$ = .09	$R^2_{Adjusted}$ = .04	$R^2_{Adjusted}$ = .21	$R^2_{Adjusted}$ = .15	$R^2_{Adjusted}$ = .09	$R^2_{Adjusted}$ = .05	$R^2_{Adjusted}$ = .21	$R^2_{Adjusted}$ = .15
	0.0010	0.00061	-0.00000020	-0.00000079	-0.0088	-0.0104	-0.000000552	0.00000136
CST	$F(2, 284) = 8.9$, $p < .001$, $R^2_{Adjusted}$ = .05	$F(2, 201) = 0.7$, $p = .50$, $R^2_{Adjusted}$ = -.003	$F(2, 284) = 9.3$, $p < .001$, $R^2_{Adjusted}$ = .05	$F(2, 201) = 1.3$, $p = .28$, $R^2_{Adjusted}$ = .003	$F(2, 284) = 5.5$, $p = .29$, $R^2_{Adjusted}$ = -.00005	$F(2, 201) = 0.6$, $p = .54$, $R^2_{Adjusted}$ = -.0004	$F(2, 284) = 9.2$, $p < .001$, $R^2_{Adjusted}$ = .05	$F(2, 201) = 7.5$, $p < .001$, $R^2_{Adjusted}$ = .06
	0.00084* **	0.00028	-0.00000014	0.000000042	-0.000528	-0.002	-0.00000104	**-0.0000104 ** **
ILF	$F(2, 289) = 14.1$, $p < .001$, $R^2_{Adjusted}$ = .08	$F(2, 202) = 5.7$, $p = .004$, $R^2_{Adjusted}$ = .04	$F(2, 280) = 43.9$, $p < .001$, $R^2_{Adjusted}$ = .23	$F(2, 202) = 17.9$, $p < .001$, $R^2_{Adjusted}$ = .14	$F(2, 289) = 11.9$, $p < .001$, $R^2_{Adjusted}$ = .07	$F(2, 202) = 4.2$, $p = .016$, $R^2_{Adjusted}$ = .03	$F(2, 289) = 41.9$, $p < .001$, $R^2_{Adjusted}$ = .22	$F(2, 202) = 17.9$, $p < .001$, $R^2_{Adjusted}$ = .14
	0.00075*	0.00065	0.00000058	0.00000037	-0.00528	-0.0036	0.00000136	0.000002
SLFP	$F(2, 288) = 8.2$, $p < .001$, $R^2_{Adjusted}$ = .05	$F(2, 203) = 3.9$, $p = .023$, $R^2_{Adjusted}$ = .03	$F(2, 288) = 47.6$, $p < .001$, $R^2_{Adjusted}$ = .24	$F(2, 203) = 21.9$, $p < .001$, $R^2_{Adjusted}$ = .17	$F(2, 288) = 12.7$, $p < .001$, $R^2_{Adjusted}$ = .07	$F(2, 203) = 1.4$, $p = .25$, $R^2_{Adjusted}$ = .004	$F(2, 288) = 47.6$, $p < .001$, $R^2_{Adjusted}$ = .24	$F(2, 203) = 21.3$, $p < .001$, $R^2_{Adjusted}$ = .17
	-0.00045	**-0.0012***	-0.00000010	-0.00000064	**0.00328** **	0.002	0.000000192	-0.00000136
SLFT	$F(2, 287) = 5.8$, $p = .003$, $R^2_{Adjusted}$ = .03	$F(2, 202) = 2.0$, $p = .14$, $R^2_{Adjusted}$ = .01	$F(2, 287) = 54.9$, $p < .001$, $R^2_{Adjusted}$ = .27	$F(2, 202) = 22.6$, $p < .001$, $R^2_{Adjusted}$ = .17	$F(2, 287) = 10.9$, $p < .001$, $R^2_{Adjusted}$ = .06	$F(2, 202) = 4.6$, $p = .011$, $R^2_{Adjusted}$ = .03	$F(2, 287) = 52.8$, $p < .001$, $R^2_{Adjusted}$ = .26	$F(2, 202) = 24.0$, $p < .001$, $R^2_{Adjusted}$ = .18
	0.00045	0.00019	0.00000056	0.00000023	**0.00544*** **	**0.00392***	0.0000012	-0.00000304
UNC	$F(2, 290) = 9.1$, $p < .001$, $R^2_{Adjusted}$ = .05	$F(2, 199) = 3.5$, $p = .033$, $R^2_{Adjusted}$ = .02	$F(2, 290) = 51.1$, $p < .001$, $R^2_{Adjusted}$ = .26	$F(2, 199) = 19.6$, $p < .001$, $R^2_{Adjusted}$ = .16	$F(2, 290) = 1.2$, $p = .32$, $R^2_{Adjusted}$ = .001	$F(2, 199) = 0.2$, $p = .79$, $R^2_{Adjusted}$ = -.008	$F(2, 290) = 49.5$, $p < .001$, $R^2_{Adjusted}$ = .25	$F(2, 199) = 20.4$, $p < .001$, $R^2_{Adjusted}$ = .16

	-0.0012* **	-0.00073	0.00000045	0.00000037	-0.00144	0.000304	0.000000296	-0.00000408

Table 3: Model 3 - Tractwise Interactions Between Length/VLR and Sex on the Relationships between Age and Microstructure

	Length (mm)		**VLR** (mm^2/mm)	
Tract	FA	MD (mm^2/sec)	FA	MD (mm^2/sec)
Fmajor	*Length:* 0.000085 *Sex(M):* -0.0025 *Age:* 0.00029 *Length*Age:* -0.0000037 *Sex(M)*Age:* 0.000011 $F(5, 487) = 2.9$, $p = .012$, $R^2_{Adjusted} = .02$	*Length:* 0.00000016 *Sex(M):* 0.000022 *Age:* 0.00000088 *Length*Age:* 0.00000000062 *Sex(M)*Age:* -0.00000032 $F(5, 487) = 18.8$, $p < .001$, $R^2_{Adjusted} = .15$	*VLR:* -0.0208 *Sex(M):* 0.0096 *Age:* -0.00456 *VLR*Age:* 0.0000392 *Sex(M)*Age:* 0.00016 $F(5, 487) = 11.6$, $p < .001$, $R^2_{Adjusted} = .10$	*VLR:* **0.0000264*** *Sex(M):* 0.000144 *Age:* **0.000016*** ** *VLR*Age:* **-0.000000576** ** *Sex(M)*Age:* -0.0000012 $F(5, 487) = 21.3$, $p < .001$, $R^2_{Adjusted} = .17$
Fminor	*Length:* 0.0011 *Sex(M):* -0.0078 *Age:* 0.0000092 *Length*Age:* -0.000014 *Sex(M)*Age:* 0.00019 $F(5, 487) = 13.7$, $p < .001$, $R^2_{Adjusted} = .11$	*Length:* 0.00000046 *Sex(M):* 0.000039 *Age:* 0.0000024 *Length*Age:* -0.0000000070 *Sex(M)*Age:* -0.00000062 $F(5, 487) = 42.7$, $p < .001$, $R^2_{Adjusted} = .30$	*VLR:* -0.00144 *Sex(M):* -0.032 *Age:* -0.00584 *VLR*Age:* -0.000104 *Sex(M)*Age:* 0.00168 $F(5, 487) = 17.0$, $p < .001$, $R^2_{Adjusted} = .14$	*VLR:* 0.0000168 *Sex(M):* 0.000232 *Age:* **0.0000224*** ** *VLR*Age:* -0.000000272 *Sex(M)*Age:* -0.00000368 $F(5, 487) = 43.8$, $p < .001$, $R^2_{Adjusted} = .30$
ATR	*Length:* 0.0031 *Sex(M):* -0.028 *Age:* 0.0018 *Length*Age:* -0.000045 *Sex(M)*Age:* 0.00055 $F(5, 491) = 3.9$, $p = .002$, $R^2_{Adjusted} = .03$	*Length:* 0.00000011 *Sex(M):* 0.000027 *Age:* 0.00000027 *Length*Age:* 0.000000028 *Sex(M)*Age:* -0.00000054 $F(5, 491) = 46.4$, $p < .001$, $R^2_{Adjusted} = .31$	*VLR:* -0.00624 *Sex(M):* -0.144 *Age:* -0.0712 *VLR*Age:* 0.000088 *Sex(M)*Age:* 0.00328 $F(5, 491) = 3.3$, $p = .006$, $R^2_{Adjusted} = .02$	*VLR:* 0.0000112 *Sex(M):* 0.000176 *Age:* **0.0000216*** ** *VLR*Age:* **-0.000000216*** *Sex(M)*Age:* -0.00000304 $F(5, 491) = 42.6$, $p < .001$, $R^2_{Adjusted} = .30$
CAB	*Length:* 0.0039 *Sex(M):* -0.019 *Age:* 0.00072 *Length*Age:* -0.000040 *Sex(M)*Age:* 0.00012 $F(5, 484) = 7.6$, $p < .001$, $R^2_{Adjusted} = .06$	*Length:* -0.00000057 *Sex(M):* 0.000030 *Age:* 0.00000028 *Length*Age:* 0.000000017 *Sex(M)*Age:* -0.00000044	*VLR:* -0.0136 *Sex(M):* 0.12 *Age:* -0.00408 *VLR*Age:* -0.00006 *Sex(M)*Age:* -0.00152 $F(5, 484) = 23.5$, $p < .001$, $R^2_{Adjusted} = .19$	*VLR:* 0.0000028 *Sex(M):* 0.000152 *Age:* 0.0000032 *VLR*Age:* 0.000000112 *Sex(M)*Age:* -0.00000312

		$F(5, 484) = 7.9$, $p < .001$, $R^2_{Adjusted} = .07$		$F(5, 484) = 15.3$, $p < .001$, $R^2_{Adjusted} = .13$
CCG	*Length:* 0.0069 *Sex(M):* -0.052 *Age:* 0.0042 *Length*Age:* -0.00011 *Sex(M)*Age:* 0.00072 $F(5, 489) = 9.3$, $p < .001$, $R^2_{Adjusted} = .08$	*Length:* 0.0000027 *Sex(M):* 0.0000091 *Age:* 0.0000040 *Length*Age:* -0.000000054 *Sex(M)*Age:* -0.00000019 $F(5, 489) = 24.9$, $p < .001$, $R^2_{Adjusted} = .19$	*VLR:* -0.00136 *Sex(M):* -0.272 *Age:* -0.0088 *VLR*Age:* -0.000144 *Sex(M)*Age:* 0.00432 $F(5, 489) = 9.4$, $p < .001$, $R^2_{Adjusted} = .08$	*VLR:* **0.000032*** *Sex(M):* -0.0000248 *Age:* **0.0000176***** *VLR*Age:* **-0.00000056*** *Sex(M)*Age:* 0.0000000168 $F(5, 489) = 26.3$, $p < .001$, $R^2_{Adjusted} = .20$
CST	*Length:* 0.0014 *Sex(M):* -0.0056 *Age:* 0.0014 *Length*Age:* -0.000014 *Sex(M)*Age:* 0.00016 $F(5, 485) = 3.7$, $p = .003$, $R^2_{Adjusted} = .03$	*Length:* 0.00000051 *Sex(M):* -0.000018 *Age:* 0.0000015 *Length*Age:* -0.0000000099 *Sex(M)*Age:* -0.00000015 $F(5, 485) = 17.9$, $p < .001$, $R^2_{Adjusted} = .15$	*VLR:* -0.00432 *Sex(M):* -0.0528 *Age:* -0.00328 *VLR*Age:* 0.0000552 *Sex(M)*Age:* 0.00144 $F(5, 485) = 0.8$, $p = .55$, $R^2_{Adjusted} = -.002$	*VLR:* -0.00000744 *Sex(M):* -0.0000688 *Age:* 0.0000024 *VLR*Age:* 0.0000000424 *Sex(M)*Age:* -0.00000184 $F(5, 485) = 20.1$, $p < .001$, $R^2_{Adjusted} = .16$
ILF	*Length:* 0.0014 *Sex(M):* -0.015 *Age:* 0.00040 *Length*Age:* -0.000012 *Sex(M)*Age:* 0.00025 $F(5, 491) = 8.3$, $p < .001$, $R^2_{Adjusted} = .07$	*Length:* 0.0000011 *Sex(M):* 0.000028 *Age:* 0.0000024 *Length*Age:* -0.000000012 *Sex(M)*Age:* -0.00000038 $F(5, 491) = 26.9$, $p < .001$, $R^2_{Adjusted} = .21$	*VLR:* -0.0152 *Sex(M):* -0.0016 *Age:* -0.0088 *VLR*Age:* 0.000184 *Sex(M)*Age:* 0.000736 $F(5, 491) = 7.0$, $p < .001$, $R^2_{Adjusted} = .06$	*VLR:* 0.00000784 *Sex(M):* 0.000208 *Age:* **0.0000136***** *VLR*Age:* -0.000000136 *Sex(M)*Age:* -0.00000264 $F(5, 491) = 26.1$, $p < .001$, $R^2_{Adjusted} = .20$
SLFP	*Length:* 0.00089 *Sex(M):* -0.025 *Age:* 0.00061 *Length*Age:* -0.000028 *Sex(M)*Age:* 0.00049 $F(5, 491) = 5.0$, $p < .001$, $R^2_{Adjusted} = .04$	*Length:* **0.0000037**** *Sex(M):* 0.000019 *Age:* **0.0000041***** *Length*Age:* **-0.000000068***** *Sex(M)*Age:* -0.00000034 $F(5, 491) = 31.2$, $p < .001$, $R^2_{Adjusted} = .23$	*VLR:* 0.00224 *Sex(M):* -0.272 *Age:* -0.004 *VLR*Age:* 0.00000704 *Sex(M)*Age:* 0.00448 $F(5, 491) = 5.3$, $p < .001$, $R^2_{Adjusted} = .04$	*VLR:* 0.00000336 *Sex(M):* 0.000136 *Age:* **0.0000136***** *VLR*Age:* -0.0000000664 *Sex(M)*Age:* -0.00000232 $F(5, 491) = 28.2$, $p < .001$, $R^2_{Adjusted} = .22$
SLFT	*Length:* 0.00048 *Sex(M):* -0.033 *Age:* -0.00012 *Length*Age:* -0.0000028 *Sex(M)*Age:* 0.00062	*Length:* 0.00000029 *Sex(M):* 0.000024 *Age:* 0.0000013 *Length*Age:* 0.0000000019 *Sex(M)*Age:*	*VLR:* -0.00144 *Sex(M):* -0.272 *Age:* -0.00616 *VLR*Age:* 0.000104 *Sex(M)*Age:* 0.00464	*VLR:* 0.00000752 *Sex(M):* 0.000152 *Age:* **0.000016***** *VLR*Age:* -0.000000144 *Sex(M)*Age:* -0.000002

	$F(5, 489) = 3.3$, $p = .006$, $R^2_{Adjusted} = .02$	-0.00000038 $F(5, 489) = 31.9$, $p < .001$, $R^2_{Adjusted} = .24$	$F(5, 489) = 6.7$, $p < .001$, $R^2_{Adjusted} = .05$	$F(5, 489) = 31.7$, $p < .001$, $R^2_{Adjusted} = .24$
UNC	*Length:* -0.00079 *Sex(M):* 0.00061 *Age:* -0.00027 *Length*Age:* -0.0000029 *Sex(M)*Age:* 0.00016 $F(5, 489) = 6.1$, $p < .001$, $R^2_{Adjusted} = .05$	*Length:* 0.0000015 *Sex(M):* 0.000018 *Age:* **0.0000022***** *Length*Age:* -0.000000018 *Sex(M)*Age:* -0.00000046 $F(5, 489) = 30.9$, $p < .001$, $R^2_{Adjusted} = .23$	*VLR:* 0.00472 *Sex(M):* -0.0112 *Age:* 0.00104 *VLR*Age:* -0.000096 *Sex(M)*Age:* 0.00128 $F(5, 489) = 1.8$, $p = .11$, $R^2_{Adjusted} = .008$	*VLR:* 0.0000144 *Sex(M):* 0.000076 *Age:* **0.0000184***** *VLR*Age:* -0.00000028 *Sex(M)*Age:* -0.00000216 $F(5, 489) = 31.0$, $p < .001$, $R^2_{Adjusted} = .23$